Bioorganic & Medicinal Chemistry Letters 21 (2011) 4215–4219

Contents lists available at ScienceDirect

Bioorganic & Medicinal Chemistry Letters

journal homepage: www.elsevier.com/locate/bmcl

Selective non zinc binding inhibitors of MMP13

Chris De Savi, Andrew D. Morley *, Attilla Ting, Ian Nash, Kostas Karabelas, Christine M. Wood, Michael James, Stephen J. Norris, Galith Karoutchi, Neil Rankine, Gordon Hamlin, Philip A. MacFaul, David Ryan, Sarah V. Baker, David Hargreaves, Stefan Gerhardt

AstraZeneca, Mereside, Alderley Park, Macclesfield, Cheshire SK10 4TG, UK

ARTICLE INFO

Article history:
Received 19 April 2011
Revised 18 May 2011
Accepted 20 May 2011
Available online 27 May 2011

Keywords:
MMP13
Selectivity
Non zinc binder
Lead Generation

ABSTRACT

Directed screening has identified a novel series of MMP13 inhibitors that possess good levels of activity whilst possessing excellent selectivity over related MMPs. The binding mode of the series has been solved by co-crystallisation and demonstrates an interesting mode of inhibition without interaction with the catalytic zinc atom.

Matrix metalloproteases (MMPs) are a class of zinc and calcium dependent endopeptidases that are responsible for the cleavage of a variety of extracellular matrix proteins.[1] More than 20 family members have been identified and these have been sub-divided dependent on their preferential substrate specificity.[2] For example, the sub group termed collagenases (MMPs 1, 8, 13, 18) have been shown to favour cleavage of various types of collagen. The enzyme family is usually tightly regulated, both at a transcription and local level,[3,4] in the latter cases via tissue inhibitors of metalloproteases (TIMPs).[5,6] However, when this equilibrium breaks down, it can lead to diseases such as arthritis, chronic obstructive pulmonary disease, cancer, periodontal disease and multiple sclerosis.[4,7–11] MMP13 (collagenase 3) has been shown to be the key enzyme in the cleavage of type II collagen and believed to play a pivotal role in the breakdown of cartilage in osteoarthritic joints.[12]

Although many inhibitors of various MMPs have been identified and progressed into clinical development, all have failed, primarily due to lack of therapeutic margins.[13,14] The rate limiting effect is musculoskeletal syndrome, which results in joint stiffness and tendonitis and the effect has been attributed to a lack of selectivity over other MMP family members. Most published MMP inhibitors contain a metal binding motif which interacts with the catalytic zinc atom, a conserved feature of the target class.[1,2,15,16] Identifying inhibitors which form enzyme specific interactions (e.g., **1** and **2**) has been shown to generate compounds with superior selectivity profiles over traditional MMP inhibitors through binding deeply in the S1′ region of MMP13.[17,18] This type of approach formed the basis for our own project strategy.

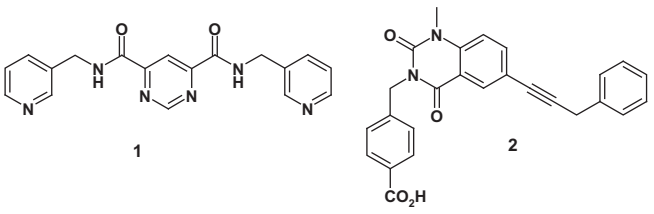

1

2

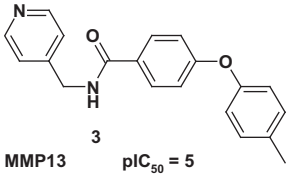

3

MMP13	pIC_{50} = 5
MMP2	pIC_{50} = 4.3
MMP9/12/14	pIC_{50} <4

A directed screen of the AstraZeneca corporate collection (19 K) against MMP13 was undertaken at 30 μM (duplicate testing), generating a 15% hit rate. Actives were tested in a four point dose response against MMPs 2, 9, 12, 13, 14 to get a view of compound potency and selectivity against key MMP isoforms.[19] A large

* Corresponding author. Tel.: +44 1509 644772.
E-mail address: andy.morley@astrazeneca.com (A.D. Morley).

0960-894X/$ - see front matter © 2011 Elsevier Ltd. All rights reserved.
doi:10.1016/j.bmcl.2011.05.075

number of non-selective inhibitors and false positives were identified as part of the downstream evaluation. One of the few compounds that did inhibit MMP13 with modest levels of selectivity was compound **3**. Binding to the enzyme was confirmed using NMR chemical shift perturbation mapping with ^{15}N-labelled MMP13 (180 μM) on a 600 MHz Varian Inova spectrometer.[20] Compound **3** induced specific amide resonance shifts in slow exchange on the NMR time scale and saturated at a 1:1 molar stoichiometry, indicative of binding in the <10 μM K_d range.

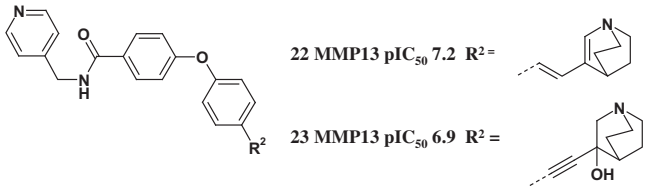

Compound **3** does not appear to be an obvious zinc binder, although the pyridine ring could be acting as a metal chelator. Alternatively, there are similarities to **1**, and a reasonable overlay can be generated.[21] Preliminary exploration focused on probing the structure activity relationship (SAR) of the amide substituent and a small set of analogues were synthesized. This initial assessment was limited due to the relatively low solubility of the compounds compared to their MMP13 potency. This made detailed evaluation at this stage risky and results were challenging to unequivocally interpret. These are summarised in Table 1.

The pyridyl or aromatic motifs *per se* are not essential for MMP13 activity. The poor potency of the unsubstituted benzyl amide (**5**) was unclear. Homologation removed MMP13 activity and methylation to generate the tertiary amide showed a slight reduction in potency. Smaller and more polar analogues, such as **10** and **12** were less active but demonstrated improved ligand efficiency (LE)[23] and/or lipophilic ligand efficiency (LLE).[24] These values were still well below what we deemed acceptable for hit identification start points. The data hinted that the compounds were inhibiting MMP13 through a novel binding mode, as the generated SAR was inconsistent with reported literature data for allosteric modulation or traditional zinc binders.[17,18]

Evaluation of the SAR of the phenoxyphenyl motif was then undertaken (Table 2). The terminal phenyl ring was required for compounds to show activity within the testing concentration range. Extending the linker between the ether and aromatic was detrimental to activity, whereas removal of the ether was tolerated, albeit with some reduction in MMP13 activity (i.e., **15**). Initial attempts from available starting materials to introduce substituents in the ortho or meta positions of the terminal ring were not encouraging, whereas para substitution was tolerated, with **21** showing the most encouraging LLEs and comparable LE to **3**.

At this stage it was essential to find some additional interactions that generated significant MMP13 potency increases to warrant progression of the series into lead identification. Based on the SAR that had been generated, a focused exploration was undertaken, around the para substituent of the terminal phenyl ring. Most of the synthesised compounds were devoid of MMP13

Table 1
Early amide SAR

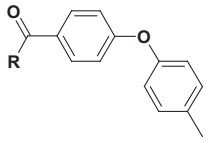

Compd	R	MMP13 pIC$_{50}$[a]	*c* Log *P*	Sol μM[b]	LE[c]	LLE[d]
3	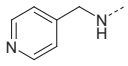	5	3.9	10	0.21	1.1
4	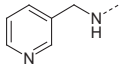	4.6	3.9	NT	0.19	0.7
5	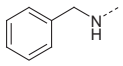	<3.4	5.4	20	—	—
6	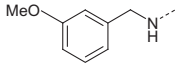	4.6	5.4	5	0.18	−0.8
7	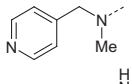	4.3	3.9	NT	0.17	1.0
8	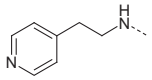	<3.4	4.0	4	—	—
9	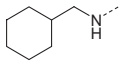	4.3	6.1	NT	0.18	−1.8
10	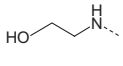	4.5	2.9	260	0.22	1.6
11	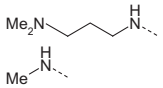	<3.4	4.1	2800	—	—
12		4.6	3.5	10	0.26	1.1

NT – Not tested.
[a] Values mean of $n = 2$ experiments.
[b] Thermodynamic solubility data.[22]
[c] LE (Ligand efficiency)[23] Values are calculated as pIC$_{50}$/Heavy atom count.
[d] LLE (Lipophilic ligand efficiency)[24] Values are calculated as pIC$_{50}$-*c* log *P*.

Table 2
Phenoxyphenyl SAR

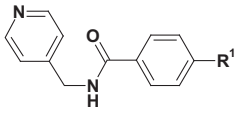

Compd	R^1	MMP13 pIC_{50}	*c* log *P*	Sol μM	LE	LLE
13	OMe	<3	1.5	2200	—	—
14	OPh	4.6	3.4	29	0.2	1.2
15	Ph	4.4	3.2	11	0.21	1.2
16		<4	3.3	9	—	—
17	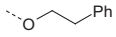	<4	3.6	35	—	—
18	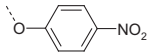	4.7	3.2	3	0.18	1.6
19	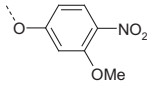	<3.4	3.1	NT	—	—
20	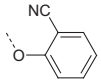	<3.4	2.9	79	—	—
21	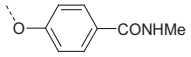	5.3	2.1	19	0.2	3.2

activity, but one analogue, **22**, provided a hundred fold improvement in potency.

In order to expand the data set around this new observation, **23** was synthesized, showing a similar MMP13 profile to **22**. Broader testing of **23** gave selectivity over MMP2 and MMP12 of 22 and 35 fold respectively, with no inhibition against a wider panel of MMPs and related metalloproteases (see supplementary information).

At this stage we were successful in co-crystallizing **23** with MMP13.[25] The (*S*)-enantiomer (**24**) preferentially bound to the enzyme in the co-crystallisation process. This preference was confirmed when both isomers were prepared[26] and tested (Table 3).

The binding mode and key interactions are summarized in Figure 1. Compound **24** binds with the majority of the molecule positioned within the S1′ pocket. Both the amide carbonyl and NH form hydrogen bonds to leucine 185 and proline 242 respectively. The diarylether fits tightly into the barrel that forms the neck of the S1′ pocket. The pyridyl motif sits in the groove where the peptide backbone of the enzyme substrate would bind, proximal to the zinc atom, but without making any specific interactions with the metal. This region of MMP13 is quite lipophilic so there are reasonable Van der Waals interactions between the aryl group of **24** with the enzyme, particularly leucine 184. The quinuclidine motif binds to the S1′ loop. This region appears to be quite flexible when comparing structures across the MMP family. The basic nitrogen forms an interaction with threonine 247, which appears to fix the loop in a specific conformation. It is assumed that lipophilic interactions between methylene units of the quinuclidine ring and proline 255 contributes to MMP13 potency. This could also play a key role in generating good selectivity over MMP2 (where the corresponding amino acid is serine). The bridgehead hydroxyl substituent is shown to form a network of hydrogen bonds with adjacent water molecules.

An approximate 4 fold difference in MMP13 activity exists between the two enantiomers. The improved MMP13 activity for the (*S*)-isomer appears the major reason for the increased MMP selectivity profile as potency for both enantiomers against the

Table 3
Enantiomeric biological profiles

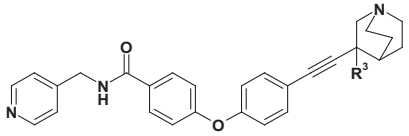

Compd	R^3	MMP13 pIC_{50}	MMP2, 9, 12, 14 fold selectivity
23	(*R*/*S*)-OH	6.9	25, >75, 35, >75
24	(*S*)-OH	7.1	94, >135, >135, >135
25	(*R*)-OH	6.5	15, >30, >30, >30

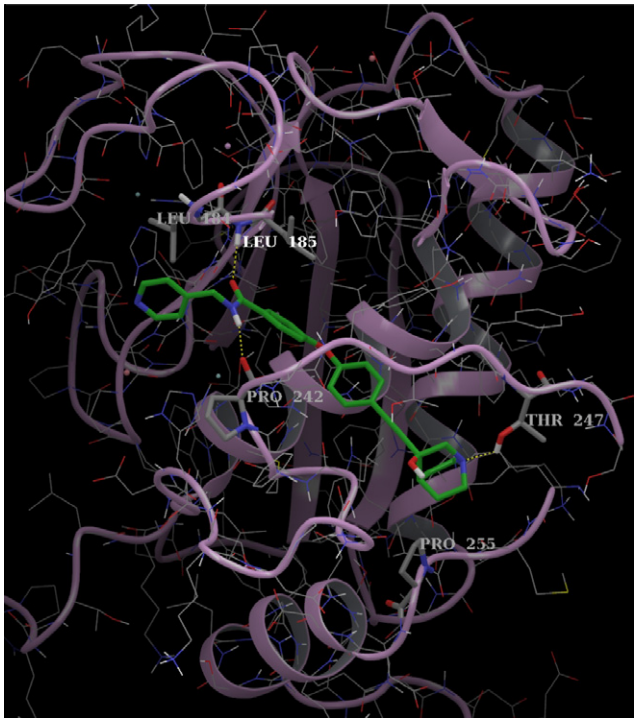

Figure 1. Structure of **24** bound to MMP13.

Table 4
Linker SAR

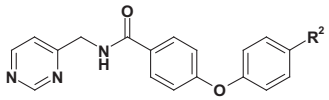

Compd	R^2	MMP13 pIC_{50}	MMP2, 9, 12, 14 fold selectivity
26	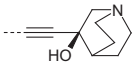	7	>100, >100, >100, >100
27	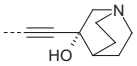	6.4	20, >25, >25, >25
28	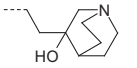	5.6	>4, >4, >4, >4
29	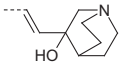	6.6	25, >40, >40, >40
30	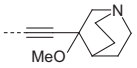	5.5	>3, >3, >3, >3
31	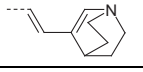	6.3	6, >20, >20, >20

Table 5
Profile of **26**

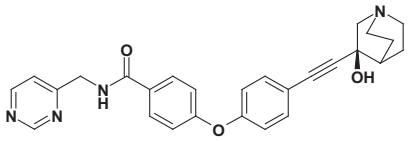

Parameter	Lead criteria	26
MMP13 pIC_{50}	pIC_{50} >7	7
MMP2, 9, 12, 14 fold selectivity	>50	>100
Cytotoxicity pIC_{50} [a]	<4.3	<4.3
Log *D*	<3.0	1.8
Mol Wt	<450	454
LE		0.21
LLE		5.1
Solubility μM[22]	>100 μM	>800 μM
Hu/Rat Prot Binding	% free	24/23
Hu Mics[b]	<30 μl/min/mg	<2 μl/min/mg
Rat Heps[c]	<15 μl/min/10^6cells	3 μl/min/10^6cells
Chem Stability[29]	$t_{½}$ >100 h	>1000 h
Cyp Inhib pIC_{50}[d]	pIC_{50} <5	<5 (5/5)
CypTDI[e]	pIC_{50} <5	<4.3 (5/5)
hERG pIC_{50}	pIC_{50} <5	<4.3
Rat PK Cl/$t_{1/2}$/V_{dss}[f]	$t_{1/2}$ >1 h	17/2.4/2.4

pIC_{50} values are the means of at least three experiments.
[a] Inhibition of THP-1 cell viability.
[b] Human microsome metabolism intrinsic clearance (μL/min/mg).[27].
[c] Rat Sprague–Dawley hepatocyte metabolism intrinsic clearance (μL/min/10^6 cells).[28]
[d] Inhibition of cytochrome P450 isoforms: 1A2, 2C9, 2C19, 2D6 and 3A4.
[e] TDI –Time dependant inhibition.
[f] Compounds dosed at 2 mg/kg iv, $n = 2$ animals (Cl ml/min/kg, $t_{1/2}$ h, V_{dss} l/kg).

other MMP isoforms is similar. Compound **24** has ~100 fold selectivity, or better, against all the family members that were tested.

The presence of the 4-pyridyl motif did mean that **23** inhibited Cyp3A4, 2C9 and 2C19 with pIC_{50}s >5. Replacing this group with a 4-pyrimidinyl unit maintained the biological profile and gave clean Cyp inhibition (pIC_{50} <5) for all isoforms tested. Attention then turned to exploring the SAR of the linker between the aryl and quinuclidine motifs in more detail. Key data is summarized in Table 4.

SAR suggests all the interactions observed in the crystal structure provide important contributions towards MMP13 activity and any modifications in this region reduced affinity and subsequently selectivity over MMP2, in particular. Several other linkers were also explored (data not shown) but all failed to generate acceptable biological profiles (MMP13 pIC_{50}s <5). Compound **26** was chosen as our lead candidate and profiled extensively (Table 5).

The presence of the alkyne unit could be perceived as a potential risk with respect to chemical reactivity (directly or via metabolites). Therefore, representative members of the series were evaluated in several stability assays to assess suitability to progress into lead optimisation. All tested analogues were stable to heating at pH range 4–10, extrapolating to $t_{1/2}$ of >1000 h in all cases.[29] No changes were observed when compounds were subjected to our in house photolytic stability assay.[30] Evaluation for reactivity in the presence of glutathione (both with and without the *S*-transferase) showed the compounds to be inert.[31] The series also showed no time dependent inhibition of five human CYPs. The electron withdrawing effects of the alkyne and oxygen functions limit the quinuclidine pK_a to 8.5, giving the series attractive physicochemical and DMPK profiles. Metabolite identification studies showed the N-oxide of the quinuclidine to be the only metabolite identified and

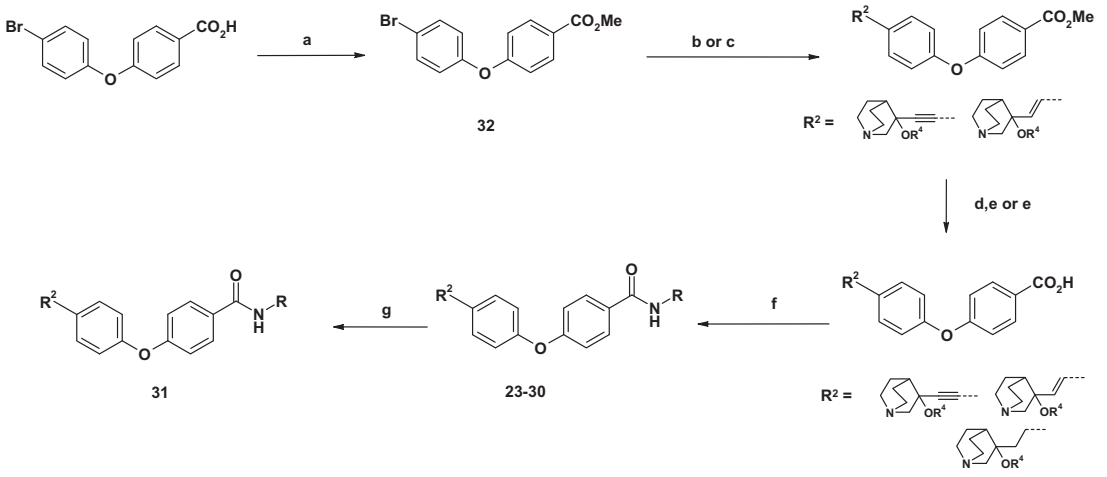

Scheme 1. Reagents and conditions: (a) 5–10% HCl/MeOH, 65 °C, 7 h, 90%; (b) quinuclidine alkyne, $Pd(Cl)_2(PPh_3)_2$, Cu(I)I, PPh_3, Et_3N, DMF, 70 °C, 83%; or (c) quinuclidine alkene, $Pd(OAc)_2$, TBACl, (*o*-tolyl)$_3$P, Et_3N, DMF, 130 °C, 1 h, MW, 59%; (d) 10% Pd/C, H_2, EtOH, 48 h, 90%; (e) 2.5 N aq NaOH (or LiOH·H_2O) H_2O/MeOH, 50 °C, 2–16 h, 84%; (f) amine, HATU, DIPEA, DMF, rt, 15–84%; (g) formic acid, 120 °C, 2.5 h, 21–96%

the profile was consistent in both rodent and human systems. The series generally scaled well from in vitro (rat hepatocytes) to rodent in vivo studies, with all tested compounds being within two fold of experimental prediction. In vivo clearances were modest and reasonable half lives were generated. Biliary and renal clearances were negligible for tested compounds. This overall profile make the series a useful start point for more detailed lead optimisation exploration.

The syntheses of key compounds are shown in Scheme 1. Intermediate, **32**, was used in palladium catalysed coupling processes to generate alkyne and alkene linkers, which can be readily reduced to the corresponding alkanes. Dehydration of the alcohol motif (OR^4) is achieved using acidic conditions to generate **31**. The synthesis of most of the exemplified quinuclidine intermediates has previously been reported.[32–34]

We have identified a novel series of selective MMP13 inhibitors and determined their binding mode through co-crystallisation studies. Compounds exert their biological effects without interaction with the catalytic zinc atom, which enables good levels of selectivity over related enzyme family members to be achieved. The series was subsequently progressed into lead optimisation and these studies will be reported in the future.

Acknowledgements

We acknowledge the work of Ben Goult in generating the NMR information and Ken Page and Gillian Smith for the TDI data.

Supplementary data

Supplementary data associated with this article can be found, in the online version, at doi:10.1016/j.bmcl.2011.05.075.

References and notes

1. Whittaker, M.; Floyd, C. D.; Brown, P.; Gearing, A. J. H. *Chem. Rev.* **1999**, *99*, 2735.
2. Hu, J.; Van den Steen, P. E.; Sang, Q.-X. A.; Opdenakker, G. *Nat. Rev., Drug Discov.* **2007**, *6*, 480.
3. Nuti, E.; Tuccinardi, T.; Rossello, A. *Curr. Pharm. Des.* **2007**, *13*, 2087.
4. Nagase, H.; Woessner, J. F., Jr. *J. Biol. Chem.* **1999**, *274*, 21491.
5. Nagase, H.; Visse, R.; Murphy, G. *Cardiovasc. Res.* **2006**, *69*, 562.
6. Gomez, D. E.; Alonso, D. F.; Yoshiji, H.; Thorgeirsson, U. P. *Eur. J. Cell Biol.* **1997**, *74*, 111.
7. Martel-Pelletier, J. *Osteoarthritis Cartilage* **1999**, *7*, 371.
8. Glodring, M. B.; Glodring, S. R. *J. Cell Physiol.* **2007**, *213*, 626.
9. Churg, A.; Wang, R. D.; Tai, H.; Wang, X.; Xie, C.; Dai, J.; Shapiro, S. D.; Wright, J. L. *Am. J. Respir. Crit. Care Med.* **2003**, *167*, 1083.
10. Hautamaki, R. D.; Kobayashi, D. K.; Senior, R. M.; Shapiro, S. D. *Science* **1997**, *277*, 2002.
11. Coussens, L. M.; Fingleton, B.; Matrisian, L. M. *Science* **2002**, *295*, 2387.
12. Mitchell, P. G.; Magna, H. A.; Reeves, L. M.; Lopresti-Morrow, L. L.; Yocum, S. A.; Rosner, P. J.; Geoghegan, K. F.; Hambor, J. E. *J. Clin. Invest.* **1996**, *97*, 761.
13. Bigg, H. F.; Rowan, A. D. *Curr. Opin. Pharmacol.* **2001**, *1*, 314.
14. Brown, P. D. *Expert Opin. Inv. Drug* **2000**, *9*, 2167.
15. Jacobsen, J. A.; Major Jourden, J. L.; Miller, M. T.; Cohen, S. M. *Biochim. Biophys. Acta* **2010**, *1803*, 72.
16. Li, N.-G.; Shi, Z.-H.; Tang, Y.-P.; Wang, Z.-J.; Song, S.-L.; Qian, L.-H.; Qian, D.-W.; Duan, J.-A. *Curr. Med. Chem.* **2011**, *18*, 977.
17. Johnson, A. R.; Pavlovsky, A. G.; Ortwine, D. F.; Prior, F.; Man, C.-F.; Bornemeier, D. A.; Banotai, C. A.; Mueller, W. T.; McConnell, P.; Yan, C.; Baragi, V.; Lesch, C.; Roark, W. H.; Wilson, M.; Datta, K.; Guzman, R.; Han, H.-K.; Dyer, R. D. *J. Biol. Chem.* **2007**, *282*, 27781.
18. Engel, C. K.; Pirard, B.; Schimanski, S.; Kirsch, R.; Habermann, J.; Klingler, O.; Schlotte, V.; Weithmann, K. U.; Wendt, K. U. *Chem. Biol.* **2005**, *12*, 181.
19. In vitro fluorescent assay for matrix metalloproteinase family including for example MMP-13: Recombinant human proMMP-13 may be expressed and purified as described by Knauper et al. [V. Knauper et al., *Biochem. J.* **1996**, *271*, 1544]. The purified enzyme was used to monitor inhibitors of activity as follows: purified proMMP-13 was activated using 1 mM amino phenyl mercuric acid (APMA) for 20 h at 35 °C in assay buffer (0.1 M tris–HCl, pH7.5, containing 0.1 M NaCl, 20 mM $CaCl_2$, 0.02 mM ZnCl and 0.05% (w/v) brij 35 containing the synthetic substrate Mca-Pro-cyclohexyl-Ala-Gly-Nva-His-Ala-Dap(Dnp)-NH2 (Bachem) in the presence or absence of inhibitors. Activity was determined by measuring the fluorescence at ex328 nm and em393 nm. An IC_{50} value for the inhibitor was calculated by plotting the raw data in a dose response curve fitting application (e.g., Origin). A similar protocol with the above substrate was used for expressed and purified pro MMP1, 2, 3, 7, 8, 9, 12, 14. Similar protocols were applied for measuring the activity of ADAM-17 and ADAM-10 using the substrate dimethoxyfluorescein-Ser-Pro-Leu-Ala-Gln-Ala-Val-Arg-ser-Ser-Arg-Cys-fluorescein (Bachem).
20. Moy, F. J.; Chanda, P. K.; Chen, J. M.; Cosmi, S.; Edris, W.; Levin, J. I.; Powers, R. *J. Mol. Biol.* **2000**, *302*, 671.
21. The model of compound **3** was built using Maestro molecular modelling program, docked using Glide into MMP13 structure (PDB ID = 1xuc) and overlay with compound **1** in Maestro. Glide and Maestro were licensed from Schrödinger, LGG (www.schrodinger.com). The final conformation of compound **3** was optimised in MMP13 protein using Szybki (MMFF94 force field) licensed from Openeye (http://www.eyesopen.com/).
22. Buttar, D.; Colclough, N.; Gerhardt, S.; MacFaul, P. A.; Phillips, S. D.; Plowright, A.; Whittamore, P.; Tam, K.; Maskos, K.; Steinbacher, S.; Steuber, H. *Bioorg. Med. Chem.* **2010**, *18*, 7486.
23. Hopkins, A. L.; Groom, C. R.; Alex, A. *Drug Discov. Today* **2004**, *9*, 430.
24. Leeson, P. D.; Springthorpe, B. *Nat. Rev. Drug. Discov.* **2007**, *6*, 881.
25. The X-ray crystal ligand–protein structure of compound **24** (PDB ID = 2YIG) has been deposited into the RCSB.
Protein data bank (http://www.pdb.org/pdb/home/home.do).
26. Coope, J. F.; Main, B. G. *Tetrahedron: Asymmetry* **1995**, *1393*, 6.
27. McGinnity, D. F.; Parker, A. J.; Soars, M.; Riley, R. J. *Drug Metab. Dispos.* **2000**, *28*, 1327.
28. Soars, M. G.; Grime, K.; Sproston, J. L.; Webborn, P. J. H.; Riley, R. J. *Drug Metab. Dispos.* **2007**, *35*, 859.
29. MacFaul, P. A.; Ruston, L.; Wood, J. M. *Med. Chem. Commun.* **2011**, *2*, 140.
30. The photolytic stability of compounds is assessed by irradiating 50 μM solution of the compounds in phosphate buffer at pH 7 in the presence of 20% ethanol co-solvent using a Hanau Suntest (Atlas Instruments) for up to 4 h. Any changes to the parent compound are assessed by LC–UV–MS. Compounds with measured half-lives of less than 30 min are regarded as being unstable.
31. MacFaul, P. A.; Morley, A. D.; Crawford, J. J. *Bioorg. Med. Chem. Lett.* **2009**, *19*, 1136.
32. Brown, G. R.; Clarke, D. S.; Foubister, A. J.; Freeman, S.; Harrison, P. J.; Johnson, M. C.; Mallion, K. B.; McCormick, J.; McTaggart, F.; Reid, A. C.; Smith, G. J.; Taylor, M. J. *J. Med. Chem.* **1996**, *39*, 2971.
33. Brown, G. R.; Hollinshead, D. M.; Stokes, E. S. E.; Clarke, D. S.; Eakin, M. A.; Foubister, A. J.; Glossop, S. C.; Griffiths, D.; Johnson, M. C.; McTaggart, F.; Mirrlees, D. J.; Smith, G. J.; Wood, R. *J. Med. Chem.* **1999**, *42*, 130.
34. Brown, G. R.; Foubister, A. J.; Freeman, S.; McTaggart, F.; Mirrlees, R. A. C.; Smith, G. J.; Taylor, M. J.; Thomason, D. A.; Whittamore, P. R. O. *Bioorg. Med. Chem. Lett.* **1997**, *7*, 597.